Triple-band HTS Filter Using Dual Spiral Resonators With Capacitive-loading

A. M. Abu Hudrouss, A. B. Jayyousi, and M. J. Lancaster

Abstract—**The increasing demand on microwave spectrum for communication systems has been the driving force in the filter industry. Multiple filtering characteristics have become necessary for many filter designs in mobile and satellite applications. In this paper, a new cost-function for an optimization algorithm to achieve multiple passband filtering function has been introduced. A High Temperature Superconductor (HTS) 10-pole filter with triple-band performance has been designed and fabricated to verify this algorithm. Each of the three passbands has a fractional bandwidth of approximately 0.26%.**

Index Terms— **bandpass filters, HTS filters, multiple-band filters, triple-band filters.**

I. Introduction

The unceasing development of telecommunication systems has led to substantial increase in their complexity and channel numbers. This initiates the need of microwave devices capable of working on multiple frequency bands. Being an essential part of such systems, microwave bandpass filters with dual-band characteristic have been designed through various approaches [1]-[10]. One report on initial work on dual band filters has simply produced two distinctive passband filters and combined them through a coupler [1]. Extra matching networks are needed at the input/output of each filter. Another method of achieving a multi-band design is to design a bandpass filter followed by stopband filter [2].

To minimize the size and the cost of the circuit, there is a trend to design a single circuit, which is capable of producing the different designated bands. Resonators with tunable 2^{nd} harmonic such as Stepped Impedance Resonators (SIRs) have been used for such purposes [3]-[6]. It is still a real challenge to synthesise the coupling coefficients and the external quality factors accurately for each of the two bands. The SIRs are usually used on dual band filters when the two bands are quite far from each other.

For close spaced passbands, other design techniques can be used such as frequency mapping transformation for the low-pass filtering function [7], [8]. These are limited to symmetric two-band cases as described in [7]. However, Macchiarella [8] introduces frequency transformation for asymmetric dual band. However, this method can be applied only when all the transmission zeros are overlapped within the middle stopband. This gives a limitation to the selectivity on the edges of the stopband. Another downside is that this method can only be applied using an inline filter, which limits the number of transmission zeros to maximum of $n/2$; where n is the order of the filter. Moreover, the reflection zeros can be only equally distributed between the two passbands regardless of their bandwidth, which results in a higher selectivity for the narrower passband at the cost of the wider band.

Optimization has been used to realize the multi-band filtering function as in [9], but for a much more general case than previously reported. However, the reflection level is not equiripple and the algorithm is restricted again to inline filters. In [10] Lee has expanded the algorithm for canonical cases enabling it to achieve $N-2$ transmission zeros; where N is the order of the filter. In both cases the cost functions for the optimization algorithms are not given.

As one of the driving points in designing multi-band filters is minimizing the size whilst preserving the performance, superconducting filters look an optimum choice. The low-loss of HTS allows very compact filters with a very small insertion loss (high sensitivity) and a sharp skirt for the filter (high selectivity). The significance of using HTS can be seen with a very narrow bandwidth for each channel; where the filters become sensitive to losses. In this paper we present the cost function for an optimization algorithm to achieve multi-band filtering function for both symmetric and asymmetrical cases. A 10-pole symmetrical triple-passband HTS filter has been designed to verify this algorithm.

II. Optimization Algorithm

The optimization algorithm, used here, aims to locate transmission and reflection zeros in such a way that realizes multi-band filtering functions. These functions are defined by the reflection losses, insertion losses, and the bandwidths for the different bands involved.

The number of reflection zeros is equal to the filter order while the number of transmission zeros depends on the filter topology. For multi-band filters, the available nulls can be evenly distributed over the different pass/stop bands (i.e. higher number of nulls for the wider bandwidth).

The following can be used:

$$Z_i = \left\lfloor \frac{BW_i . X}{\sum_{k=1}^{p} BW_k} \right\rfloor \quad (1)$$

Where Z_i is the number of nulls assigned to each band *i*, BW_i is the bandwidth of band *i*, and *p* is the total number of passbands or stopbands within the response. X refers to the maximum number of available nulls. It equals the number of resonators when considering passbands and it equals the number of transmission zeros in case of stopbands. As Z_i is rounded to the lowest nearest integer, the number of assigned zeros can be less than the filter order. The missing nulls can be allocated arbitrarily to any of the available stop/pass-bands.

The error function depends on the ripple-peak values of S_{11} and S_{21} within the passbands and stopbands respectively. The summation of the difference between the attained ripple-peak values and the desired ripple-peak values is calculated at every iteration and compared to an arbitrary small number; the value of which depends on the required accuracy.

The optimization starts with arbitrary chosen nulls the ripple-peak values can be evaluated through the following procedure.

Starting with a single passband filtering function, the scattering parameters can be written as:

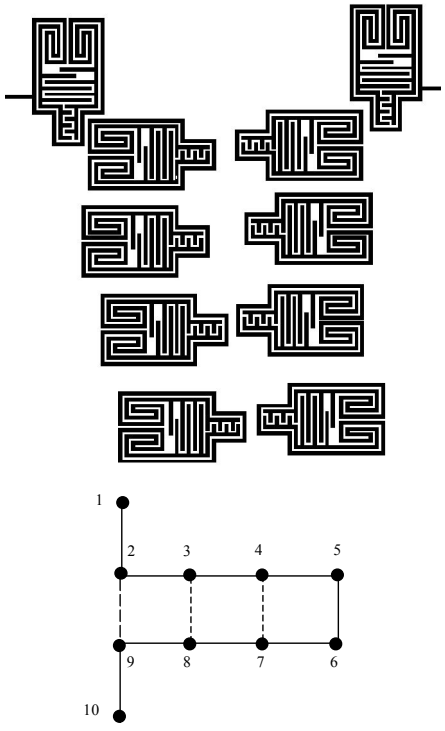

Fig. 2. Layout of a 10-pole microstrip filter (diagram is not to scale)

$$\left|S_{21}(j\Omega)\right| = \frac{1}{1+\delta * C_n(\Omega)} \quad (2)$$

and

$$\left|S_{11}(j\Omega)\right| = \frac{1}{1+1/(\delta * C_n(\Omega))} \quad (3)$$

Where Ω represents a radian frequency variable of a lowpass prototype filter with unity cutoff frequency, the constant δ is the nominal ripple, and $C_n(\Omega)$ is the filtering function, defined as:

$$C_n(\Omega) = \frac{P(\Omega)}{F(\Omega)} \quad (4)$$

Where $F(\Omega)$ and $P(\Omega)$ are polynomials whose roots are the frequency positions of the reflection and the transmission nulls respectively. Because of the multiband nature of the filtering functions under consideration, the nominal ripple does not directly correspond to the equal ripple of any of the passbands. To underline this fact, the common symbol of ε is replaced by δ as seen in equation (2) and (3).

The value of nominal ripple can be found through the optimization process along with the locations of the required nulls.

Substituting for $C_n(\Omega)$ in (1) and (2) and taking the derivatives with respect to Ω will lead to:

$$\frac{dS_{11}}{d\Omega} = \frac{(P.F' - P'.F)}{\delta(P/\delta + jF)^2} \quad (5)$$

$$\frac{dS_{21}}{d\Omega} = \frac{P.F' - P'.F}{j(P + j\delta.F)^2/\delta} \quad (6)$$

The arguments of the polynomials are dropped for convenience. From (5) and (6), it is clear that the numerators of the derivatives are equal. This leads to the conclusion that the maxima and minima of both functions occur at the same frequency.

It should be noted that when considering stopbands, reflection-loss maxima are ignored. Likewise, when considering passbands, insertion-loss maxima should be neglected.

The cost function can be formulated as:

$\Omega = A + B$

Where:

$$A = \sum_{k=1}^{g}\left[\sum_{i=1}^{z(k)}\left|S_{11}(x_i^k) - S_{11\max}^{\ k}\right|\right] \quad (7)$$

and

$$B = \sum_{k=1}^{n}\left[\sum_{i=1}^{m(k)}\left|S_{21}(y_i^k) - S_{21\min}^{\ k}\right|\right] \quad (8)$$

The variables *x* and *y* corresponds to the reflection and insertion ripple-peak frequency locations respectively. The constant *g* in the outer summation of (7) corresponds to the number of required passbands, whereas *n* corresponds to the number of stopbands. The internal summation in both

equations is carried out for nulls within a single band. $z(k)$ and $m(k)$ corresponds to the number of maxima within the k^{th} passband and stopband respectively . $S_{11}^{\max}$ is the designated value of maximum reflection loss within the k^{th} passband. Likewise $S_{11\min}^{k}$ is the designated insertion loss within the k^{th} stopband.

Some constraints need to be taken into consideration to avoid convergence to local minima. The most important of these involves restricting nulls to their assigned bands. Considering a certain band, k, with a bandwidth extends from f_1 to f_2, and assuming that $\{x_1, x_2 \ldots x_m\}$ are the initially assigned nulls for that stop/pass band, the nulls position can be rescaled at the outset of each optimization iteration using:

$$\overline{x_i} = f_1 + \frac{f_2 - f_1}{x_m - x_1}(x_2 - x_1) \qquad (9)$$

Where $\overline{x_i}$ is the position of the i^{th} null following the rescaling procedure.

Moreover, nulls located at the edges of each band can be allowed to move during the optimization within a certain tolerance. The smaller this tolerance is, the more accurate the realized bandwidths are. However, this usually comes at the price of degrading the equi-ripple level sought within each band. A compromise needs to be established based on which of the two parameters is of more importance to the filter designer. The term edge-null tolerance will be used to refer to the percentage of the bandwidth within which the edge nulls of any band can be located.

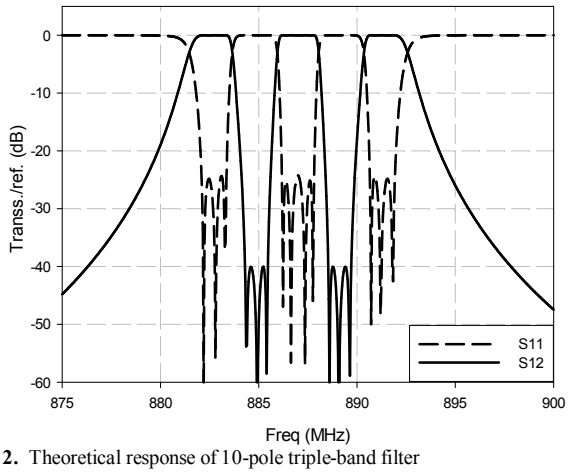

Fig. 2. Theoretical response of 10-pole triple-band filter

III. Triple –Band Filter

A 10-pole filter with designated centre frequency 887 MHz and total bandwidth of 11.5 MHz has been designed to have a triple-band. Each stop/pass band has a bandwidth of 2.3 MHz, an insertion loss for the stopband of –40 dB, and a reflection loss for the passband of -25 dB. The optimization algorithm requires 90 iterations to realize the positions of the reflection and transmission zeros which are given in table I. To achieve the prescribed rejection levels, the bandwidth tolerance has been chosen to be 30 %. This results in a decrease for two the terminal passbands of 7.1% each. The centre passband has been realized as specified. The achieved transmission/reflection losses are depicted in Fig. 2. In getting the transfer functions (S_{11} and S_{12}), the general coupling matrix can be constructed using the synthesis method developed by Cameron [11]. To achieve the six required transmission zeros with 10 resonators, semi-canonical topology (fig 2.b.) has been chosen; where the cross couplings are between the 2nd and 9th, 3rd and 8th, and 4th and 7th resonators. To achieve this topology from the general form of coupling matrix, the matrix has been synthesized using the SFG model

TABLE I
REFLECTION AND ATTENUATION ZEROS FOR THE 10TH ORDER TRIPLE-PASSBAND FILTER

K	1	2	3	4	5	6	7	8	9	10
R. Z.	-0.9607	-0.8394	-0.7431	-0.1527	-.0685	.0685	0.1527	0.7431	0.8394	0.9607
T. Z.	-0.5251	-0.4148	-0.3185	0.3185	0.4148	0.5251				

TABLE II
COUPLING MATRIX FOR THE 10TH ORDER TRIPLE-PASSBAND FILTER

	1	2	3	4	5	6	7	8	9	10
1	0	0.7827	0	0	0	0	0	0	0	0
2	0.7827	0	0.5597	0	0	0	0	0	0.2048	0
3	0	0.5597	0	0.3451	0	0	0	0.0637	0	0
4	0	0	0.3451	0	0.2372	0	0.4454	0	0	0
5	0	0	0	0.2372	0	0.3058	0	0	0	0
6	0	0	0	0	0.3058	0	0.2372	0	0	0
7	0	0	0	0.4454	0	0.2372	0	0.3451	0	0
8	0	0	0.0637	0	0	0	0.3451	0	0.5597	0
9	0	0.2048	0	0	0	0	0	0.5597	0	0.7827
10	0	0	0	0	0	0	0	0	0.7827	0

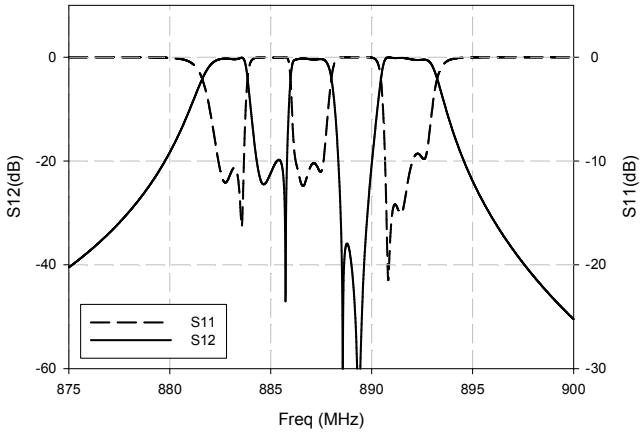

Fig. 3. EM simulated response of 10-pole triple-band HTS filter

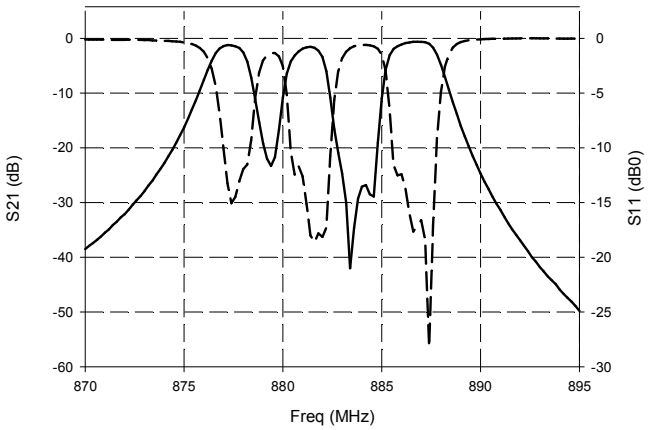

Fig. 4. Measured response of 10-pole triple-band HTS filter

developed by Jayyousi [12]. Table II gives the resultant matrix. Input and output external quality factors both take a value of 1.7338.

IV. Filter Fabrication

Figure 2b shows a layout of the 10-pole canonical filter. The basic resonator is the compact double-spiral inductor resonator developed by Zhou [13]. Not only does the resonator have a very compact structure, but it also holds most of the electric and magnetic energy near the surface of the substrate. This makes the spurious coupling between non-adjacent resonators very weak. The centre frequency of the resonators is also immune to the small fluctuation in the substrate thickness. Moreover, spiral resonators in general are less sensitive to over-etching during manufacturing [14].

The filter design was carried out according to the coupled-resonators design methodology, which is well covered in the literature [15]. The external quality factors were converted into a distance between the feed-line and virtual ground of the resonator. The direct and cross couplings were also converted into spacing between the corresponding resonators.

The substrate is MgO with thickness of 0.5 mm and the chip size is 40 mm × 20 mm using YBCO thin film on both sides of the substrate. The resonator line width is 50 μm. The filter has been simulated and optimized using sonnet software with resolution of 50 μm × 50 μm. The simulated response is shown in Fig. 3. The discrepancy between simulated and theoretical responses may be attributed to the spurious coupling between diagonal pairs of resonators in the folded canonical structure and the limitation on cell size of the grid.

V. Measurement Results

The circuit has been patterned onto the substrate, which is bonded onto a Mgo carrier fixed in a titanium box. Both the carrier and the box were covered by 6 μm thick gold. Dielectric screws have been used for tuning the filter. The tuning screws give limited control over the resonant frequency for each resonator. Hence, they allow compensation for errors in coupling coefficients and external quality factors. Due to the high number of resonators in the filter, the tuning was tedious with the lack of a sophisticated tuning algorithm.

Instead of having one passband as normal filters, the filter has 3 passbands and 2 stopbands which need to be tuned simultaneously. The resultant total bandwidth after tuning is 11.3 MHz with discrepancy of 0.2 MHz to the designed one; the passbands are 1.8 MHz, 1.7 MHz, and 2.5 MHz.

The experimental result is depicted in Fig. 4. The centre frequency is shifted down by 4.85 MHz from the simulated response. This can be explained by limitation of software or/and defects in various levels of the fabrication. However, apart from the frequency shift, there is good agreement between the measured and simulated results in Fig. 3. and Fig. 4.

The losses on the passbands are mainly due to the small fractional bandwidth of each passband, which is approximately 0.26%. A small bandwidth results in high sensitivity to small shift of resonant frequency of the resonators.

VI. Conclusion

A novel triple-band HTS filter was presented in this study. An algorithm which allows design of multiple band symmetric and asymmetric filtering function is also provided. The measured results agree with the simulated ones. However, the filter exhibits problems concerning tuning. More advanced tuning algorithms can be used in the future for higher accuracy.

ACKNOWLEDGEMENT

The authors would like to thank D. Holdom for patterning the HTS circuit, P. Suherman for her help and Mr C. Ansell for his technical support.

REFERENCES

[1] H. Miyake, S. Kitazawa, T. Ishizaki, and T. Yamada and Y. Nagatami "A miniaturized monolithic dual band filter using ceramic lamination technique for dual mode portable telephones," in IEEE MTT-S International Microwave Symposium Digest, vol 2, June1997, pp 789–792.

[2] L.-C Tsai, C.-W. Hsue, "Dual-band bandpass filters using equal-length coupled-serial-shunted lines and Z-transform technique," IEEE Trans. on Microwave theory and Tech., vol. MTT-52, pp 1111-1117, April 2004.

[3] S. –F. Chang, Y. –H. Jeng, and J. -L. Chen, "Dual-band step-impedance bandpass filter for multimode wireless LANs," Electronic Letters, vol. 40, pp 38-39, Jan. 2004.

[4] H.-M. Lee, C.-R. Chen, C.-C Tsai, and C. –M. Tsai, "Dual-band coupling and feed structure for microstrip filter design," IEEE MTT-S International Microwave Symposium Digest, vol 3, pp 1971-1974, June 2004.

[5] S. Sun, L. Zhu, "Coupling dispersion of Parallel-coupled microstrip lines for dual-band filters with controllable fractional pass bandwidths," IEEE MTT-S International Microwave Symposium Digest, pp 2195-2198,June 2005.

[6] J. –T. Kuo, T. –H. Yeh, C. –C Yeh, "Design of microstrip bandpass filters with a dual-passband response" IEEE trans. on Microwave theory Tech., vol. MTT-53, pp 1331-1337, April. 2005.

[7] R. J. Cameron, M. Yu, and Y. Wang, "Direct-coupled microwave filters with single and dual stopbands," IEEE trans. Microwave theory Tech., vol. MTT-53, pp 3288-3297, Nov. 2005.

[8] G. Macchiarella, S. Tamiazzo, " Design Techniques for Dual-passband filters," IEEE trans. on Microwave theory Tech., vol. MTT-53, pp 3265-3271, Nov. 2005.

[9] S. Holme, " Multiple passband filters for satellite applications," Proc. 20th AIAA Int. Communications Satellite Systems conf. Exhibit, 2002.

[10] J. Lee , M. Seok, I. –B. Yom, " A dual-passband filter of canonical structure for satellite applications," IEEE Microwave and Wireless Component Letters, vol. 14, pp 271-273, June 2004.

[11] J. C. Cameron, "Advanced coupling matrix synthesis techniques for microwave filters," IEEE trans. on Microwave theory Tech., vol. MTT-51, pp 1-10, Jan. 2003.

[12] A. B. Jayyousi, M. J. Lancaster, F. Huang, "On the synthesis of cross-coupled resonators filters," IEEE Trans. on Microwave Theory Tech., submitted for publication.

[13] J. Zhou, M. J. Lancaster, and F. Huang " Superconducting microstrip filters using compact resonators with double-spiral inductors and interdigital capacitors," IEEE MTT-S International Microwave Symposium Digest, vol 3, pp 1889-1892, June 2003.

[14] F. Huang, "Ultra-compact superconducting narrow-band filters using single- and twin-spiral resonators," IEEE Trans, on Microwave Theory Tech., vol. MTT-51, pp 487-491, Feb. 2003.

[15] J. –S. Hong, M. J. Lancaster, "Microstrip filters for RF/microwave applications," John Wiley & Sons, Inc. 2001, ch. 8.

[16] EM User's Manual, Sonnet Software Inc., Version 6, 1999.

[17] C. Quendo, E. Rius, and C. Person, "An original topology of dual-band filter with transmission zeros," IEEE MTT- S International Microwave Symposium Digest, pp 1093-1096, June 2003.

Ammar M. Abu-Hudrouss was born in Kanyounis, Palestine in 1977. He received the BSc degree from Islamic University Gaza, Palestine in 1995. He received the Msc degree in Communication Engineering in 2003 and PhD in Microwave Engineering in 2007; both from Birmingham University, Birmingham, UK.
He is currently an assistant professor at Islamic University of Gaza, Palestine. His current research interest is discrete-time signal processing and microwave planar filters.

Awni Jayyousi received the BSc degree from the University of Jordan , Amman , Jordan , in 2001, and the MSc degree in telecommunications engineering and PhD in microwave engineering from the University of Birmingham , Birmingham , UK , in 2002 and 2006, respectively. He is currently an assistant professor at the University of Amman, Jordan. His current research is centered on microwave filter design and sensitivity analysis, in addition to wireless energy transfer."

Michael J. Lancaster (M'91) was educated at Bath University, UK, where he graduated with a degree in Physics in 1980. His career continued at Bath , where he was awarded a PhD in 1984 for research into non-linear underwater acoustics.
After leaving Bath University Prof Lancaster joined the surface acoustic wave (SAW) group at the Department of Engineering Science at Oxford University as a research fellow. The research was in the design of new, novel SAW devices, including filters and filter banks. In 1987 he became a lecturer at The University of Birmingham in the Department of Electronic and Electrical Engineering, lecturing in electromagnetic theory and microwave engineering. Shortly after he joined the department he began the study of the science and applications of high temperature superconductors, working mainly at microwave frequencies. Prof. Lancaster was promoted to head the Emergining Deveice Technology Research Centre in 2000 and head of the department of Electronic, Electrical and Computer Engineering in 2003. His present personal research interests include microwave filters and antennas, as well as the high frequency properties and applications of a number of novel and diverse materials.